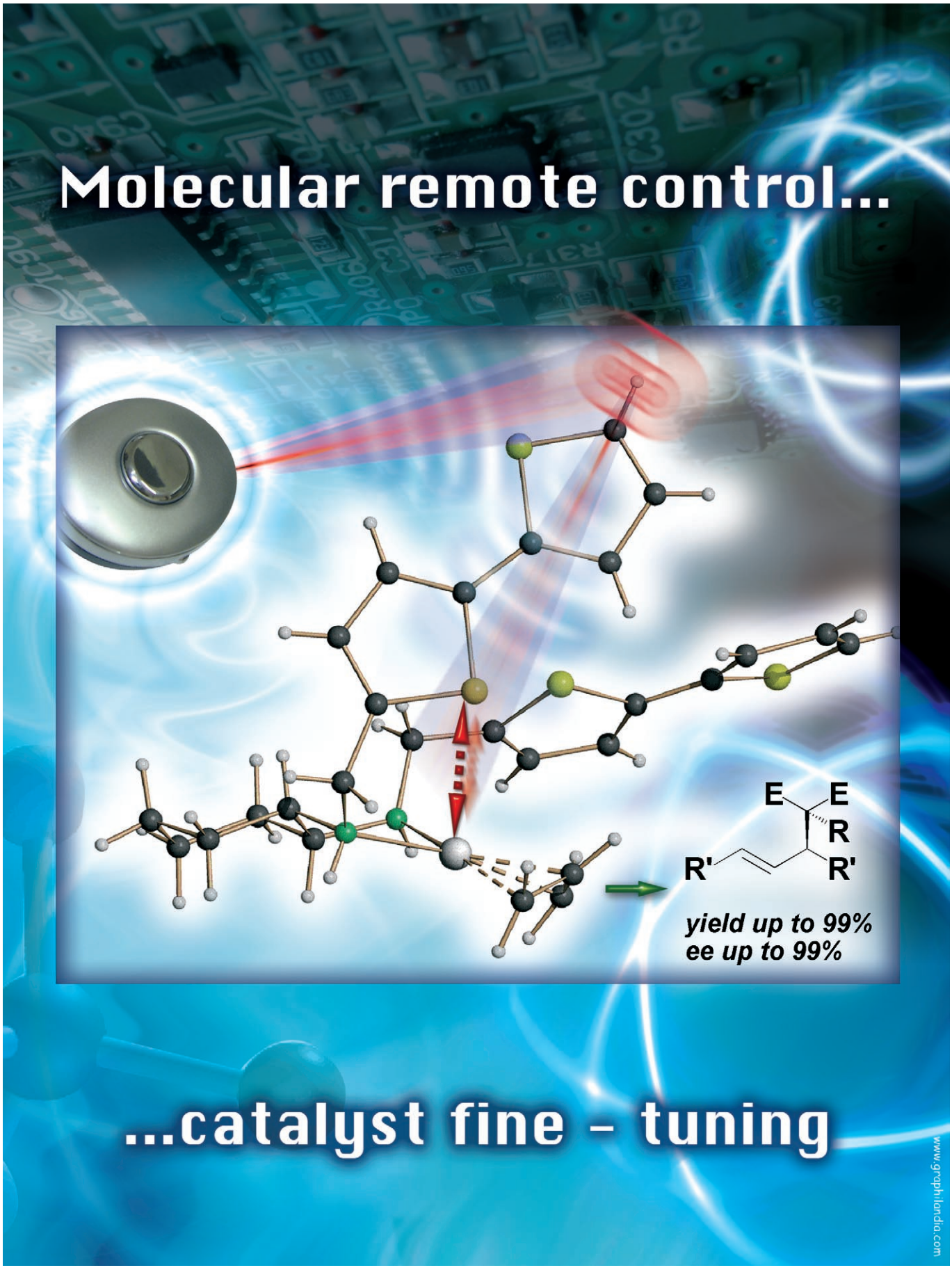

CHEMISTRY
A EUROPEAN JOURNAL

DOI: 10.1002/chem.200500889

Controlling Stereochemical Outcomes of Asymmetric Processes by Catalyst Remote Molecular Functionalizations: Chiral Diamino-oligothiophenes (DATs) as Ligands in Asymmetric Catalysis

Vincenzo Giulio Albano,[a] Marco Bandini,*[a] Giovanna Barbarella,[b] Manuela Melucci,[b] Magda Monari,[a] Fabio Piccinelli,[a] Simona Tommasi,[a] and Achille Umani-Ronchi*[a]

Abstract: The synthesis, characterization, and structure-guided application of a new class of highly versatile chiral C_2-symmetric diamine-oligothiophene ligands in Pd-catalyzed asymmetric transformations are presented. Experimental investigations of the intimate role of pendant π-conjugate oligothiophenes in determining the catalytic activity of the corresponding chiral Pd complexes are described. Their unusual behavior opens up new routes toward the logical design of finely tuned organometallic catalysts by remote structural functionalizations.

Keywords: asymmetric catalysis · electronic interactions · palladium · thiophenes · X-ray diffraction

Introduction

Asymmetric catalysis has blossomed over the last six decades.[1] Tremendous progress has been made toward the development of new catalytic protocols for the facile synthesis of ever more challenging stereochemically defined, enantiopure compounds (EPCs) in pharmacology, agrochemicals, and materials science.[2] In this context, the search for new, effective, chiral organic molecules to control the stereochemical outcomes of organic transformations is a long-sought goal of numerous synthetic chemists. Generally, the overall performances of chiral organometallic catalysts are the result of reciprocal and synergic influences between the catalaphoric (metal center) and chiraphoric (ligand) units. Among these, the nature of coordinating atoms present in the ligand framework affects the catalytic activity of the metal center significantly. Variations in the electronic features of the coordinating atoms as well as modifications of the ligand skeleton in the proximity of the metal center are among the most commonly adopted strategies to control both chemical and optical yields in asymmetric transformations. In some cases, however, these are difficult to accomplish, due to poor tolerance by the ligands of harsh oxidative/reductive conditions and lack of structural flexibility in the ligand skeletons; therefore, the fine-tuning of the catalytic performances of the chiral species through remote backbone functionalization would be preferable.[3] In this context, Gilheany and Bunt's results are noteworthy: they reported elegantly on the possibility of modulating the performances of Cr–salen and Pd–PHOX (asymmetric epoxidation of alkenes, and asymmetric allylic alkylation, respectively), simply by choosing the substitution pattern of the arene rings in the chiral ligands appropriately.[4]

While the design of new stereodiscriminating systems has frequently dealt with biological stereoselective transformations (that is, enzyme-based cascade sequences),[5,6] it is interesting that the interchange of know-how between organometallic asymmetric catalysis and hybrid organic–inorganic materials disciplines[7] remains poorly explored.

Theoretically, the π-conjugate system of oligoaryl compounds, which is fundamental for several modern electro-optical devices, guarantees an ideal pattern throughout the structural backbone and the coordinated metal.[8] In this field, oligothiophene molecular motifs are of pivotal importance,[9] because of their ready synthetic accessibility and unusual coordinating features that allow transition metals to

[a] Prof. Dr. V. G. Albano, Dr. M. Bandini, Prof. Dr. M. Monari, Dr. F. Piccinelli, Dr. S. Tommasi, Prof. Dr. A. Umani-Ronchi
Dipartimento di Chimica "G. Ciamician"
Università di Bologna
Via Selmi 2, 40126 Bologna (Italy)
Fax: (+39) 512-099-456
E-mail: marco.bandini@unibo.it
achille.umanironchi@.unibo.it

[b] Dr. G. Barbarella, Dr. M. Melucci
CNR-ISOF
Via Gobetti 101, 40129 Bologna (Italy)

couple conveniently to the organic backbone with consequent modulation of their overall electro-optical properties.[10] Of particular relevance is the affinity of functionalized thienyls and oligothienyls for Pd^{II} salts; this has been widely exploited for the synthesis of inner-sphere architectural-type hybrid organic–inorganic materials.[11] All of these considerations make chiral oligothiophene structural motifs potentially useful also for the design of fine-tunable stereoselective organometallic catalysts (Figure 1).

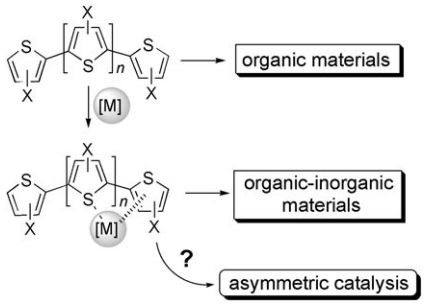

Figure 1. Chiral oligothiophene catalysts for asymmetric catalysis inspired by materials science.

We have reported recently the synthesis, chemo-optical characterization, and catalytic properties of a new family of chiral ligands containing oligothienyl systems (diamino-oligothiophenes, DATs) that proved effective in the stereoselective Pd-catalyzed asymmetric allylic alkylation (AAA)[12] of allylcarbonates.[13]

The presence of a sizable intramolecular interaction between the apparently spectator ancillary inner thienyl rings through the sulfur atom and the metal center suggests interesting guidelines for the design, prediction, and fine-tuning of the catalytic activity of chiral organometallic species simply by conveniently engineering the electronic features of the thienyl side arm; we call this approach molecular remote control (MRC).

We do not intend to add this class of ligands to the already rich collection of valuable auxiliaries for this transformation. On the contrary, we wish to highlight and to prove the remarkable effect of their intramolecular "weak/secondary" interactions on the stereochemical outcome of asymmetric catalytic processes.

Results and Discussion

In the course of our continuing efforts to develop new chiral organometallic catalysts for enantiodiscriminating transformations, we reported recently on the synthesis of a family of chiral C_2-symmetric multidentate diamino-oligothiophenes (DATs, **3a**,**b**).[13,14] DATs were readily obtainable through reductive amination of commercially available (*R*,*R*)-1,2-cyclohexanediamine (**1**) by the corresponding thienyl (T) aldehydes **2a**,**b** (Scheme 1). Then DATs **3a**,**b** were successfully employed in a bench-test reaction for new chiral auxiliaries

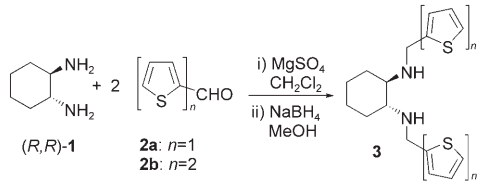

Scheme 1. Synthesis of DATs **3a**, **b**: i) (*R*,*R*)-**1** (1.0 equiv), **2** (2.0 equiv), $MgSO_4$ (10.0 equiv), CH_2Cl_2, RT, 32 h; ii) $NaBH_4$ (5.0 equiv), MeOH, RT, 16 h.

in late-transition metal chemistry, namely asymmetric allylic alkylation. Although extensive literature already addresses this transformation with aromatic hindered substrates (**4a**,**b**),[12,15] the search for broadly effective chiral ligands on more challenging aliphatic unhindered allylic substrates is still ongoing.

With model malonates **5a** and **b** (Table 1), excellent levels of chemical ($\leq$99%) as well as optical (*ee* up to 99%) yields were obtained with **3b** in the presence of aromatic

Table 1. DAT ligands in the Pd-catalyzed allylic substitution with carbonate **4**: proving the role of the thienyl rings.[a]

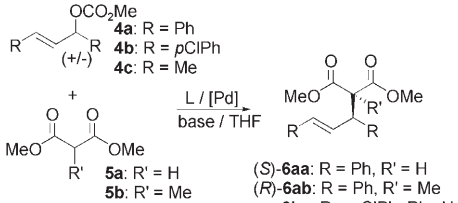

Entry	L	Conditions[b]	Product	Yield [%][c]	*ee* [%][d]
1	**3a**	A	**6aa**	65	45 (*S*)
2	**3b**	A	**6aa**	96	99 (*S*)
3	**3b**	A	**6ab**	80	>98
4	**3b**	A	**6ba**	99	95 (*R*)
5	**3b**	B	**6ca**	98	80 (*S*)
6	**3b**	B	**6ca**	40	90 (*S*)[e]

[a] All the reactions were carried out under a nitrogen atmosphere at RT (16 h). [b] Conditions: A) $[Pd_2(dba)_3]\cdot CHCl_3$, BSA, KOAc; B) $[Pd(allyl)Cl]_2/Cs_2CO_3/AgSbF_6$. [c] After flash chromatography. [d] Determined by chiral HPLC for **6aa** and **6ba**, chiral GC for **6ca**, and ^1H NMR with $[Eu(hfc)_3]$ for **6ab**. The absolute configuration was assigned by comparison with the known optical rotation value. [e] Reaction time 4 d at 0°C.

carbonates **4a** and **4b**. Remarkably high also was the enantiodiscrimination achieved with **3b** in the presence of the dimethyl methylmalonate **5b**, which afforded (*R*)-**6ab** in 80% yield as a single enantiomer (*ee*>98% by chiral shift ^1H NMR, entry 3, Table 1). Then we tested the effectiveness of our ligand of choice, **3b**, with the more challenging dimethylallyl carbonate **4c**. After a brief survey of experimental conditions, both yield and enantiomeric excess in (*S*)-**6ca** could be increased, to 98 and 80%, respectively, using $[Pd(\eta^3\text{-}C_3H_5)Cl]_2/AgSbF_6$/**3b** (0.05:0.1:0.1, entry 5) as the catalytic system. Again, to improve the enantioselectivity in **6ca**

further, the influence of the temperature was investigated. In particular, when the model reaction was run at 0 °C, although the reaction rate dropped (yield 40 %, entry 6), the enantiomeric excess reached 90 %.

Crystallographic evidence on $[Pd(\eta^3\text{-}C_3H_5)(\mathbf{3b})]^+$ provided insight into the role of thiophene rings in the stereochemical outcome of the process. In particular, one inner thiophene was found to interact attractively with the transition-metal center [S2···Pd 3.34(1) Å].[13] On the basis of the experimental findings previously reported,[13] we hypothesized the presence of such a hemilabile contact[16] in solution also, dynamically bringing the oligothienyl side arm closer to the catalaphoric unit with increased overall stereodifferentiation. It is noteworthy that AAA processes have already proven to be strongly affected in solution, even by "weak/secondary" intramolecular contacts between side arms of the ligand and metal center.[17]

We thought that the well-known ability of oligothiophenes to shuttle charges across their organic backbone would offer the opportunity of fine-tuning the electronic (coordinating) properties of the inner sulfur atom and the catalytic activity of the corresponding Pd complex, simply by modifying the ligand skeleton even in positions remote from the metal-bonding heteroatoms (that is, by molecular remote control, MRC).[18]

In this context, the easily accomplishable electronic alteration of oligothienyls, by grafting electron-releasing or -withdrawing substituents, would make MRC a potentially useful and versatile tool for fine-tuning of the catalyst for several chiral organometallic promoted reactions.

To properly control and assess the role of the electronic interactions in modulating the catalytic activity of the metal center, we synthesized a series of 5″-functionalized, enantiomerically pure T_2 ligands (**3c–f**) in moderate to good overall yields (31–55 %), starting from the corresponding aldehydes **2c–f** (Scheme 2).

To verify the overall changes of electronic distribution in these ligands, we analyzed and compared UV/Vis spectra of ligands **3b–f** (Figure 2a). Here, the π–π bands in the ligand exhibited a red-shift absorption that increased progressively along with the electron-donating group (EDG) strength (λ_{abs} (CH_2Cl_2): **3c** 411(271) nm, **3b** 312 nm, **3d** 317 nm, **3e** 326 nm, **3f** 371 nm) due to the well-known ability of electron-releasing groups to increase the HOMO level of π-conjugate systems. Of particular relevance is the maximum absorbance at 411 nm shown by T_2NO_2 (**3c**) that can be associated with a charge-transfer absorption band.[19] In addition to this absorbance (typical for molecules that behave as push–pull systems),[20] **3c** showed also a weak band at 271 nm that may be correlated with the intense bands recorded for **3b**,**d–f** spanning 312–371 nm.

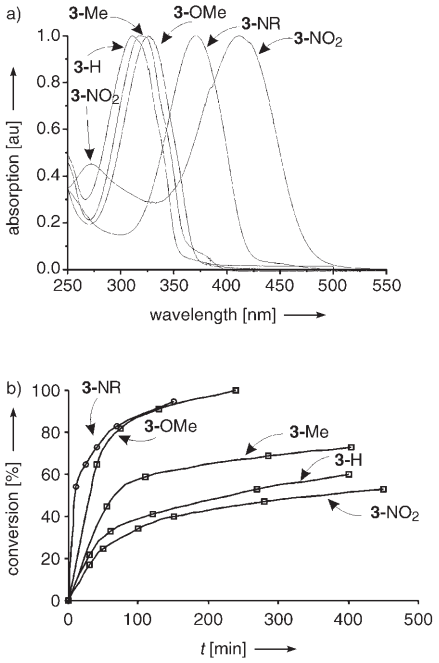

Figure 2. a) UV/Vis spectra for **3b**, **c–f** recorded in CH_2Cl_2. b) Conversion profiles in the Pd-catalyzed AAA between **4a** and **5a** for variously substituted DATs.

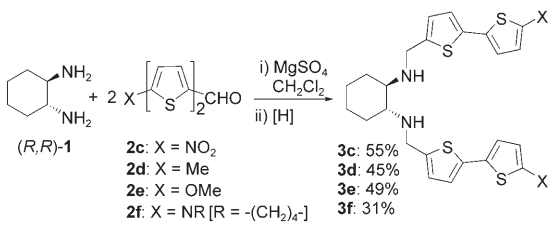

Scheme 2. i) (*R*,*R*)-**1** (1.0 equiv), **2** (2.0 equiv), $MgSO_4$ (10.0 equiv), CH_2Cl_2, RT, 48 h; ii) [H]**2c**: $NaBH_3CN$ (3.0 equiv), HCl_{dry} in Et_2O (2.0 equiv), THF, 0 °C→RT, 16 h; [H]**2d–f**: $NaBH_4$ (5.0 equiv), MeOH, RT, 16 h.

The end-capped ligands (*R*,*R*)-**3c–f** were then tested under the optimized conditions in the model reaction (**4a** + **5a**). The results are summarized in Table 2: apart from **3c**, containing the nitro group (*ee* 60 %, entry 1), all the ligands furnished **6aa** with comparable high enantioselectivity (97–99 %). However, markedly different reaction rate profiles were observed over the range of ligands (Figure 2b). Here, a good correlation between reaction rate and substitution pattern of the bithienyl pendants was observed, with a rate increasing progressively with the electron-donating character of the thiophene substituent (NR > OMe > Me > H > NO_2). In particular, the initial reaction rate with T_2NR (**3f**, R = $-(CH_2)_4-$), bearing the strongest EDG, was estimated to be approximately 1.6, 2.1, 2.6, and 3.9 times that of T_2MeO (**3e**), T_2Me (**3d**), T_2H (**3b**), and T_2NO_2 (**3c**), respectively. These results are fully in agreement with Zheng and coworkers' recent study on the dependence of AAA outcomes on the electronic features of the P,N ligand.[21]

This distinctive behavior was even more evident for the less sterically hindered carbonate **4c** (Table 2). Indeed, when DATs bearing ever-increasing electron-donating end-caps were used, both yield and enantiomeric excess of **6ca** increased, with yields in the range 20–50 % and *ee* values of 68–92 %.[22] Besides the marked increase in chemical yield

Table 2. Application of functionalized DATs **3** in AAA.

Entry	**3**	**6aa**		**6ca**	
		Yield [%][a]	*ee* [%][b]	Yield [%][a]	*ee* [%][c]
1	**3c**	75	60 (*S*)	20	68 (*S*)
2	**3b**	96	99 (*S*)	40	90 (*S*)
3	**3e**	98	99 (*S*)	42	91 (*S*)
4	**3f**	98	99 (*S*)	50	92 (*S*)
5	**3g**	98	98 (*S*)	–[d]	–

[a] After flash chromatography Reaction conditions: (**6aa**) [$Pd_2(dba_3)$]·$CHCl_3$, BSA, KOAc; (**6ca**) $[Pd(allyl)Cl]_2/AgSbF_6/Cs_2CO_3$]. [b] Determined by chiral HPLC. The absolute configuration was assigned by comparison with the known optical rotation value. [c] Determined by chiral GC. The absolute configuration was assigned by comparison with the known optical rotation value. [d] See ref. [22].

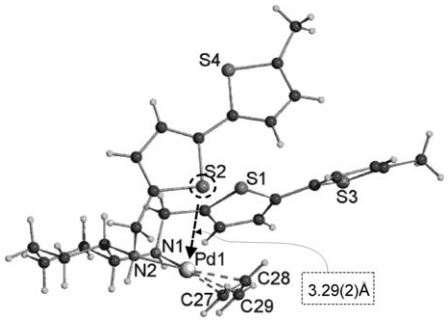

Figure 3. Molecular structure of the cation $[Pd(\eta^3\text{-}C_3H_5)(\mathbf{3d})]^+$ as the BF_4^- salt, determined by X-ray diffraction. Selected bond lengths (Å): Pd1–C27 2.109(9) Pd1–C28 2.10(1), Pd1–C29 2.144(7), Pd1–N1 2.117(5), Pd1–N2 2.144(4), C27–C28 1.35(2), C28–C29 1.35(2), Pd···S2 3.293(2).

for **6ca**, our attention was also attracted by the narrow trend in the relative *ee* value*s*, which can be rationalized in terms of the peculiar electronic as well as steric properties of these organometallic catalysts. Here, the presence of electron-releasing groups on the pendant oligothienyls, by favoring the attractive character of the thienyl–metal interaction, should shorten the S–Pd contact, with consequent higher steric congestion in the proximity of the metal center. To support this assumption, **3d** was treated with $[Pd(\eta^3\text{-}C_3H_5)Cl]_2/AgBF_4$ to give $[Pd(\eta^3\text{-}C_3H_5)(\mathbf{3d})]BF_4$ in a straightforward manner (95% yield).

The overall conformation of the $[Pd(\eta^3\text{-}C_3H_5)(\mathbf{3d})]^+$ cation is similar to that of $[Pd(\eta^3\text{-}C_3H_5)(\mathbf{3b})]^+$, exhibiting opposite absolute configurations of the coordinated nitrogen atoms [(*S*)-N1; (*R*)-N2] and λ conformation of the five-membered palladacycle (Figure 3). It is noteworthy that the contact between S2 and Pd is significantly shorter than that in $[Pd(\eta^3\text{-}C_3H_5)(\mathbf{3b})]^+$ [(3.293(2) Å against 3.340(1) Å)], fully supporting our hypothesis regarding the influence of remote substituents on the catalyst activity.

The remarkable connections between chemical outcomes and electronic features of the ligand were further highlighted by synthesizing the diamino compound **3g**, in which the inner thienyl rings were replaced by the strongly electron-donating 3,4-ethylenedioxythiophene (EDOT, Scheme 3).[23] Our choice was dictated by the distinctive effects of EDOT units embedded in oligoaryl systems. These structural motifs generally lead to pronounced flattening of π-conjugate systems, with consequent superior electron-releasing properties of the hetero-substituted thienyl rings.[24] Interestingly, under optimal reaction conditions, **3g** allowed (*S*)-**6ca** to be isolated with a remarkably higher yield (73%) and excellent *ee* (94%). To the best of our knowledge, this result represents one of the highest levels of stereoinduction obtained so far with unhindered aliphatic acyclic substrate **4c**.[25]

To gain more insight into this unusual behavior we needed to shed light on the reaction mechanism. For this purpose, the pre-catalytic species $[Pd(\eta^3\text{-}1,3\text{-}Ph_2C_3H_3)(\mathbf{3b})]BF_4$ was also synthesized in quantitative yield (95%) as an air-stable complex, starting from **3b** and $[Pd(\eta^3\text{-}1,3\text{-}Ph_2C_3H_3)Cl]_2$. In the *syn*,*syn* isomer molecule (Figure 4), the central carbon of the allyl moiety points upward (pseudo-*exo* type) and no disorder was detected. We attempted to identify the actual species present in solution by liquid ^1H NMR analysis of the $[Pd(\eta^3\text{-}1,3\text{-}Ph_2C_3H_3)(\mathbf{3b})]BF_4$ over a range of temperatures and with different solvents. In the collected ^1H NMR spectra (RT, CD_2Cl_2) coalescence of the signals of the allyl protons (*anti*) was observed. However, at −20 °C the spectrum showed two sets of signals that have been assigned to the *syn*,*syn*-pseudo-*exo* and *syn*,*syn*-pseudo-*endo* isomers (1.6:1) by the allyl *J*(H,H) coupling constants.[26] When the temperature was still lower (−50 °C)

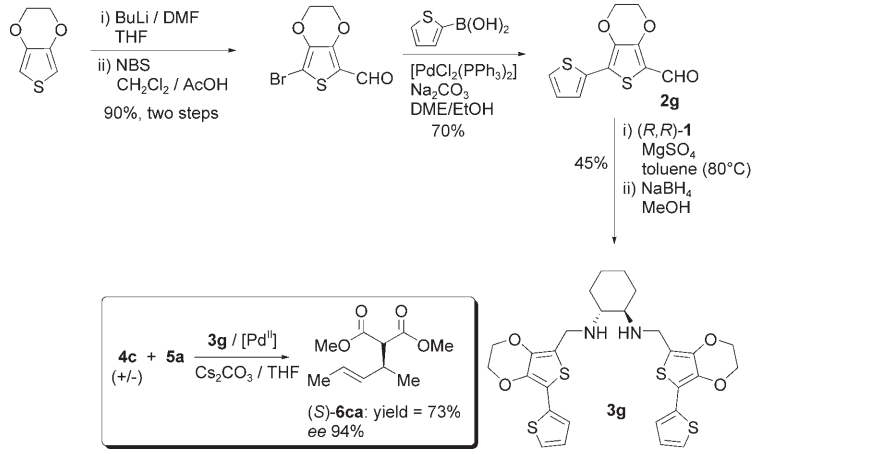

Scheme 3. Synthesis of AEDOT-T (**3g**) and its application in the AAA between **4c** and **5a**: i) EDOT (1 equiv), *n*BuLi (2.5 M, 1 equiv), −78 °C→0 °C (over 20 min) → −78 °C, then DMF (1.9 equiv), RT, 1 h; ii) EDOT-CHO (1 equiv), *N*-bromosuccinimide (1 equiv), CH_2Cl_2/AcOH 1:1, 0 °C, 2 h (in the dark) 95%. **2g**: $[PdCl_2(PPh_3)_2]$ (3 mol%), Na_2CO_3 (5 equiv), DME/EtOH 1:1, 50 °C, 16 h. **3g**: i) (*R*,*R*)-**1** (1.0 equiv), **2g** (2.0 equiv), $MgSO_4$ (10.0 equiv), toluene, 80 °C, 48 h; ii) $NaBH_4$ (5.0 equiv), MeOH, RT, 16 h, 45% (two steps).

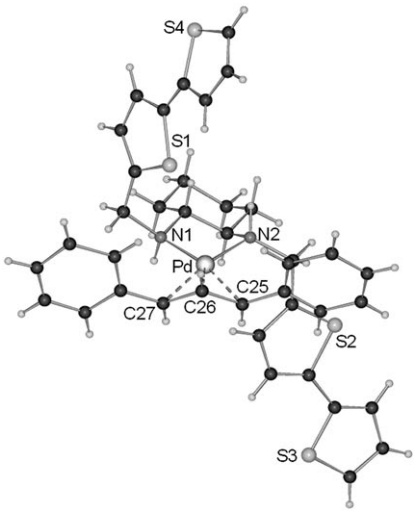

Figure 4. Molecular structure of the cation $[Pd(\eta^3\text{-}1,3\text{-}Ph_2C_3H_3)(\mathbf{3b})]^+$ as the BF_4^- salt, determined by X-ray diffraction. Selected bond lengths (Å): N1–Pd 2.14(1), N2–Pd 2.15(1), Pd–C25 2.21(1), Pd–C26 2.11(2), Pd–C27 2.19(1), Pd···S1 3.443(5).

a shift of the pseudo-*exo*–*endo* equilibrium toward the thermodynamic pseudo-*exo* species was recorded (2.8:1). As expected, the solvent drastically affected the Pd–allyl species exchange. Yet attempts to reveal the presence of minor isomers in the reaction solvent ([D_8]THF) failed. In fact, over the temperature range studied (25→−90 °C), only one set of NMR signals was observed. This finding can be ascribed to the presence in solution of a single isomer (pseudo-*exo*) or to a rapid exchange between the two isomeric Pd complexes on the NMR time-scale.

The close contact between the thienyl sulfur and the palladium center is still present in the $[Pd(\eta^3\text{-}1,3\text{-}Ph_2C_3H_3)(\mathbf{3b})]^+$ crystal structure [(S2···Pd 3.44(1) Å)], with the bithiophene ancillary arm occupying a pseudo-axial position. The thienyl-containing pendant that does not interact intimately with Pd adopts an axial orientation in order to minimize the steric congestion with the more encumbering phenyl groups. In contrast to the crystal structures in Figure 3, both nitrogen atoms of the ligand adopt an *S* configuration. The molecular geometry shows that the palladium is almost symmetrically bonded to the allyl termini: [Pd–C25 2.21(1) Å, Pd–C27 2.19(1) Å], with consequently similar electronic surroundings for C25 and C27. This evidence tends to exclude the operation of an early transition state[27] during the nucleophilic attack and, as already discussed elsewhere, the preferential rotation (PR) model should be applied in order to justify the overall stereoinduction of the chiral Pd catalyst.[28] Therefore, a rationale for the absolute stereochemistry emerges from comparison of the energies of the corresponding $[Pd^0\text{-}\|]$ species represented schematically in Scheme 4,[29] in which the differently oriented pendant thiophene groups are indicated by black and gray spots. In particular, while the bithiophene interacting with the Pd (black spot) points above the organic framework, the second pendant (gray spot) has a spatial arrangement almost parallel to the 1,3-diphenylallyl unit (Figure 4). If nucleophilic attack is postulated to occur on C1, the counterclockwise rotation will operate in order to orient the C–C double bond properly with respect to the palladium center. Contrarily, a clockwise rotation should be considered for a hypothetical nucleophilic attack on C3. While strong steric interaction of the pendant thiophene groups with the allyl unit will prevent the clockwise movement, nucleophilic attack on C1, producing a less sterically hindered rotation of the Pd-coordinated product, will result as the favored stereochemical pathway.

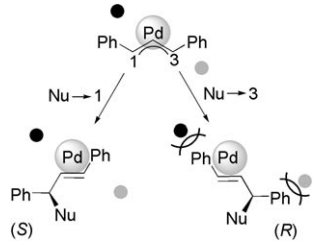

Scheme 4. Rationale of the *S* absolute configuration obtained on the basis of the preferential rotation (PR) model.

On the basis of these considerations, the observed overall increase in reaction rate with higher electron density should be rationalized in terms of electronic $[Pd^0\text{-}\|]$ stabilization. As sulfur atoms have a well-known tendency to interact strongly with soft metals,[30] we may speculate that the observed thiophene–metal interaction could contribute to stabilization of the Pd^0 intermediate complexes. In fact, the increased electron population of the sulfur atoms caused by introducing EDGs will contribute to the overall stabilization of the entire complex as well as that of the reaction transition state. In support of this last statement, secondary interactions between coordinating functional groups and Pd^0 species (the proximity effect) have been reported recently to be crucial in the transition state stabilization of Pd-catalyzed cross-coupling reactions.[31]

Conclusion

In this work we have described the synthesis, characterization, and application in AAA of a new class of chiral oligothienyl ligands. The high efficiency of intramolecular delocalization of their π-electrons calls for possible fine-tuning of the catalytic properties through "remote control" groups. In particular, the unusual trends in the chemical and stereochemical outcomes recorded for the probe reaction suggest the presence in solution also of the key attractive intramolecular contact recorded in the solid state.

In view of the simplicity of the ligand–catalyst assembly, the employment of the present "molecular remote control" model for the development of new catalytic stereoselective transformations appears to be promising and is currently under investigation.

Experimental Section

General methods: All reactions were performed in a dry nitrogen atmosphere using standard Schlenk techniques. Anhydrous solvents and reagents were purchased from Fluka and Aldrich, and used as received. We recorded ^{1}H NMR and ^{13}C NMR spectra on a Gemini Varian 200 (200 MHz) or Gemini Inova 300 (300 MHz) spectrometer. GC-MS spectra were recorded with a Hewlett-Packard 5971 instrument. LC-electrospray ionization mass spectra were obtained with an Agilent Technologies MSD1100 mass spectrometer. IR analysis was performed with an FT-IR Nicolet 205, and HPLC with a Hewlett-Packard HP1100 equipped with a chiral column (Chiralcel OD/AD). Analytical GC was performed on a Hewlett-Packard HP6890 gas chromatograph using a chiral Megadex-5 (25 m) column. Melting points were determined with a Büchi 150 melting point unit and are not corrected. The UV/Vis spectrophotometer was a Perkin-Elmer model 554.

Synthesis of 2c–g

Compound 2c: Prepared by Suzuki coupling ($[PdCl_2(PPh_3)_2]/Na_2CO_{3(aq)}$/dimethoxyethane/EtOH/50 °C, 95 % yield) between commercially available 5-nitro-2-bromothiophene and 5-formyl-2-thiopheneboronic acid. Purified by flash chromatography (*c*-hex/AcOEt 7:3→6:4): yellow-orange solid; m.p. 139–141 °C; ^{1}H NMR (200 MHz, $CDCl_3$, 25 °C, TMS): δ = 9.94 (s, 1H), 7.90 (d, J = 4.4 Hz, 1H), 7.75 (d, J = 4.0 Hz, 1H), 7.43 (d, J = 4.0 Hz, 1H), 7.28 (d, J = 4.4 Hz, 1H); ^{13}C NMR (50 MHz, $CDCl_3$, 25 °C, TMS): δ = 182.5, 151.9, 147.0, 146.1, 144.4, 136.8, 129.5, 126.8, 124.7; IR (Nujol): $\tilde{\nu}$ = 2926(s), 2853(m), 1732(s), 1660(m), 1461(s), 1335(w), 1209(m) cm^{-1}; UV/Vis (MeOH): λ_{abs} = 340 nm; MS (70 eV): *m*/*z* (%): 239 (100), 209 (10), 149 (50), 121 (20).[32]

Compound 2d: Prepared by Suzuki coupling ($[Pd(PPh_3)_4]/K_2CO_3$/toluene/MeOH/reflux) of commercially available 5-methyl-2-thiopheneboronic acid and 5-bromothiophenecarboxaldehyde.[32]

Compound 2e: Prepared by Stille coupling ($[Pd(PPh_3)_4]$/THF/reflux, 85 % yield) of 5-methoxy-2-tributyltinthiophene[33] and 5-bromothiophenecarboxaldehyde.[34]

Compound 2f: Prepared by Stille coupling ($[Pd(PPh_3)_4]$/toluene/reflux, 70 % yield) of 5-pyrrolidine-2-tributyltinthiophene and 5-bromothiophenecarboxaldehyde.

Compound 2g: Prepared by Suzuki coupling ($[PdCl_2(PPh_3)_2]/Na_2CO_3$/DME/EtOH/50 °C, 70 % yield). Purified by flash chromatography: white solid; R_f = 0.33 (*c*-hex/AcOEt 8:2); m.p. 135–137 °C; ^{1}H NMR (200 MHz, $CDCl_3$, 25 °C, TMS) δ = 9.92 (s, 1H), 7.44–7.46 (m, 1H), 7.39 (d, J = 1.6 Hz, 1H), 7.09 (t, J = 4.2 Hz, 1H), 4.44 (s, 4H); ^{13}C NMR (50 MHz, $CDCl_3$, 25 °C, TMS): δ = 179.3, 148.6, 136.8, 133.3, 127.5, 126.8, 125.8, 114.7, 97.1, 65.2, 64.7; IR (Nujol): $\tilde{\nu}$ = 3002(m), 1648(s), 1.520(m), 1488(m), 1463(s), 1373(m), 1271(m) cm^{-1}; UV/Vis (MeOH): λ_{abs} = 370 nm; MS (70 eV): *m*/*z* (%): 252 (68), 156 (18), 127 (100), 111 (33), 69 (55).

(1*R*,2*R*)-*N*,*N*′-Bis(thienylmethyl)cyclohexane-1,2-diamines (3)

Typical procedure: The desired aldehyde **2** (2 mmol) and (1*R*,2*R*)-diaminocyclohexane **1** (1 mmol) were dissolved in dry CH_2Cl_2 (10 mL) under an N_2 atmosphere in a two-necked flask (50 mL). $MgSO_4$ (5 mmol) was added and the mixture was stirred at RT for 24–48 h (checked by ^{1}H NMR). The solution was filtered on Celite and the solvent was removed under vacuum. The crude diimine was diluted with cyclohexane and stirred overnight. The purified insoluble product was collected by filtration.

(*R*,*R*)-T$_2$NO$_2$ (3c): HCl (2 mmol, 1 M in Et_2O) was added to a cooled solution (0 °C) of diimine (1 mmol) in THF (5 mL). The resulting orange slurry was stirred for 10 min, then $NaBH_3CN$ (3 mmol) was added. The clear solution was allowed to warm at RT and stirred overnight. Then water (10 mL) was added, MeOH was evaporated, and the product was extracted with CH_2Cl_2 (3×4 mL). Evaporation of the volatiles afforded crude **3c**, which was purified by flash chromatography: deep brown solid; R_f = 0.33 (CH_2Cl_2/MeOH 99:1); yield 55 % (two steps); m.p. 119–121 °C; $[\alpha]_D$ = −9.3 (*c* = 0.95 in $CHCl_3$); ^{1}H NMR (200 MHz, $CDCl_3$, 25 °C, TMS): δ = 7.78 (d, J = 5.6 Hz, 2H), 7.21 (d, J = 3.6 Hz, 2H), 7.00 (d, J = 3.6 Hz, 2H), 6.35 (d, J = 3.4 Hz, 2H), 4.15 (d, J = 14.8 Hz, 2H), 3.94 (d, J = 14.8 Hz, 2H), 2.37–2.40 (m, 2H), 1.50–1.82 (br, 4H), 1.10–1.35 (br, 4H); ^{13}C NMR (75 MHz, $CDCl_3$, 25 °C, TMS): δ = 24.7, 31.5, 45.3, 60.7, 121.7, 125.5, 126.3 (2C), 129.7, 133.5, 145.7, 149.3; IR (Nujol): $\tilde{\nu}$ = 3286(w), 3104(w), 2926(s), 2849(s), 2351(w), 1604(w), 1515(m), 1493(m), 1465(s), 1327(s), 1249(m), 1094(s), 795(s) cm^{-1}; UV/Vis (CH_2Cl_2): λ_{abs} = 271, 411 nm; elemental analysis calcd (%) for $C_{24}H_{24}N_4O_4S_4$ (560.73): C 54.41, H 4.31, N 9.99; found: C 54.45, H 4.33, N 10.00.

Compound 3d–f: $NaBH_4$ (5 mmol) was added in portions to a cooled solution (0 °C) of diimine (1 mmol) in MeOH (5 mL), and the mixture was stirred at RT until the diimine had disappeared completely (checked by ^{1}H NMR). Then water (10 mL) was added, MeOH was evaporated, and the product was extracted with CH_2Cl_2 (3×4 mL). Evaporation of the volatiles afforded crude **3**, which was purified by consecutive washings or flash chromatography.

(*R*,*R*)-T$_2$Me (3d): Purified by flash chromatography: pale yellow solid; R_f = 0.30 (CH_2Cl_2/MeOH 99:1); yield 45 % (two steps); m.p. 77–78 °C; $[\alpha]_D$ = +8.1 (*c* = 0.42 in $CHCl_3$); ^{1}H NMR (200 MHz, $CDCl_3$, 25 °C, TMS): δ = 6.90 (t, J = 3.6 Hz, 4H), 6.75 (d, J = 3.6 Hz, 2H), 6.61 (d, J = 3.6 Hz, 2H), 4.08 (d, J = 14.2 Hz, 2H), 3.86 (d, J = 14.2 Hz, 2 Hz), 2.47 (s, 6H), 3.32–2.37 (m, 2H), 1.55–1.88 (m, 4H), 1.12–1.38 (m, 4H); ^{13}C NMR (75 MHz, $CDCl_3$, 25 °C, TMS): δ = 143.1, 138.6, 136.7, 135.4, 126.8, 125.2, 123.2, 122.4, 60.1, 45.4, 31.2, 24.9, 15.3; IR (Nujol): $\tilde{\nu}$ = 3280(w), 3000(w), 2921(s), 2853(s), 1695(w), 1462(m), 1376(m), 1262(w), 1097(m), 1022(m), 789(m) cm^{-1}; UV/Vis (CH_2Cl_2): λ_{abs} = 317 nm; elemental analysis calcd (%) for $C_{26}H_{30}N_2S_4$ (498.79): C 62.61, H 6.06, N 5.62; found: C 62.58, H 6.01, N 5.60.

(*R*,*R*)-T$_2$MeO (3e): Used without further purification; pale beige solid; yield 49 % (two steps); m.p. 76–77 °C; $[\alpha]_D$ = +15.0 (*c* = 1.22 in $CHCl_3$); ^{1}H NMR (200 MHz, $CDCl_3$, 25 °C, TMS): δ = 6.78–6.83 (m, 4H), 6.72 (d, J = 3.6 Hz, 2H), 6.07 (d, J = 4.2 Hz, 2H), 4.09 (d, J = 14.2 Hz, 2H), 3.90 (s, 6H), 3.85 (d, J = 14.2 Hz, 2H), 2.33–2.39 (m, 2H), 1.65–1.88 (br, 4H), 1.20–1.56 (br, 4H); ^{13}C NMR (50 MHz, $CDCl_3$, 25 °C, TMS): δ = 165.1, 142.4, 136.7, 124.8, 124.2, 121.6, 120.8, 104.3, 60.3, 60.2, 45.7, 31.5, 24.9; IR (Nujol): $\tilde{\nu}$ = 3291(w), 2921(s), 2846(s), 2362(w), 1572(w), 1540(m), 1508(m), 1456(s), 1386(m), 1196(w), 1062(w), 793(w) cm^{-1}; UV/Vis (CH_2Cl_2): λ_{abs} = 326 nm; elemental analysis calcd (%) for $C_{26}H_{30}N_2O_2S_4$ (530.79): C 58.83, H 5.70, N 5.28; found: C 58.79, H 5.65, N 5.26.

Compound 3f, 3g: The imine precursors were synthesized as described in the typical procedure by reaction in toluene at 80 °C (24 h).

(*R*,*R*)-T$_2$NR (3f): Purified by flash chromatography: pale brown solid; R_f = 0.31 (CH_2Cl_2/MeOH 98.5:1.5); yield 31 % (two steps); m.p. 80–82 °C; $[\alpha]_D$ = +56.6 (*c* = 0.5 in $CHCl_3$); ^{1}H NMR (300 MHz, $CDCl_3$, 25 °C, TMS): δ = 6.83 (dd, J = 2.4, 4.2 Hz, 2H), 6.72–6.84 (m, 4H), 5.61 (dd, J = 2.1, 4.2 Hz, 2H), 4.09 (d, J = 14.1 Hz, 2H), 3.84 (d, J = 14.1 Hz, 2H), 3.26–3.29 (m, 8H), 2.32–2.35 (m, 2H), 2.18–2.20 (m, 4H), 2.02–2.12 (m, 8H), 1.72–1.75 (2H), 1.21–1.25 (m, 2H); ^{13}C NMR (75 MHz, $CDCl_3$, 25 °C, TMS): δ = 154.9, 141.2, 138.3, 125.3 (2C), 123.9, 120.7, 120.0, 100.5, 66.1, 60.4, 51.0, 45.8, 26.0, 25.2; IR (neat): $\tilde{\nu}$ = 3283(w), 3058(w), 2936(m), 2851(m), 1558(w), 1535(s), 1505(s), 1481(s), 1456(m), 1352(m), 1054(m), 739(m) cm^{-1}; UV/Vis (CH_2Cl_2): λ_{abs} = 371 nm; elemental analysis calcd (%) for $C_{32}H_{40}N_4S_4$ (608.21): C 63.12, H 6.62, N 9.20; found: C 63.17, H 6.57, N, 9.19.

(*R*,*R*)-EDOT-T (3g): Purified by flash chromatography: white solid; R_f = 0.32 (CH_2Cl_2/MeOH 9:1); yield 45 % (two steps); m.p. 50–52 °C; $[\alpha]_D$ = +40.0 (*c* = 0.38 in $CHCl_3$); ^{1}H NMR (300 MHz, $CDCl_3$, 25 °C, TMS): δ = 7.13–7.16 (m, 2H), 6.95–6.98 (m, 2H), 4.27–4.29 (m, 4H), 4.19–4.22 (m, 4H), 3.95 (d, J = 15.2 Hz, 2H), 3.73 (d, J = 15.2 Hz, 2H), 2.28–2.31 (m, 2H), 2.15 (pseudo d, J = 12.9 Hz, 2H), 2.00 (br, 4H), 1.72–1.75 (m, 2H); ^{13}C NMR (75 MHz, $CDCl_3$, 25 °C, TMS): δ = 138.2, 137.1, 135.0, 127.0, 123.2, 122.4, 114.5, 109.7, 65.0, 64.6, 60.2, 41.2, 31.3, 24.9; IR (neat): ν = 3424(s), 2924(s), 2846(m), 1643(m), 1534(m), 1436(s), 1362(m), 1088(s) cm^{-1}; LC-ESI-MS: *m*/*z*: 587 $[M+H]^+$; elemental analysis calcd (%) for $C_{28}H_{30}N_2O_4S_4$ (586.11): C 57.31, H 5.15, N 4.77; found: C 57.28, H 5.12, N 4.76.

Pd-catalyzed AAA (4c/5a): A two-necked flask (25 mL) was charged, under a nitrogen atmosphere, with $[Pd(allyl)Cl]_2$ (2.7 mg, 7.5×10^{-3} mmol), diamine **3g** (8.8 mg, 0.015 mmol), and anhydrous THF

(500 μL). While the mixture was being stirred at room temperature for 15 min, a white solid was formed. The subsequent addition of $AgSbF_6$ (0.015 mmol, 5 mg) dissolved the white solid and the solution turned brown. After a few minutes' stirring (with formation of solid AgCl), **4c** (24 μL, 0.15 mmol) was added, the reaction flask was cooled at 0 °C and dimethyl malonate (0.75 mmol, 86 μL) and Cs_2CO_3 (0.3 mmol, 99 mg) were added sequentially. The reaction was stirred for four days, then quenched with a saturated solution of $NaHCO_3$ (3 mL). The two phases separated and the aqueous phase was extracted with AcOEt (3×5 mL). The organic layers were collected, dried over Na_2SO_4, then concentrated. The desired product, (*S*)-**6ca**, was isolated as a yellow oil in 73% yield (22 mg) after flash chromatography (*c*-hex/AcOEt 95:5). The *ee* of the product (94%) was determined by GC with a chiral column (flow rate 15 mL min^{-1}; 50 °C for 6 min, ramp @ 1 °C min^{-1} to 180 °C); $t_R(S)$ = 42.7 min; $t_R(R)$ = 43.0 min; $[\alpha]_D$ = −15.0 (*c* = 0.34 in $CHCl_3$), lit. (*S*)-**6ca** $[\alpha]_D$ = −27.9 (*c* = 1.1 in $CHCl_3$).[36]

[Pd(η^3-C_3H_5)(3d)]BF_4: In a Schlenk flask, flamed and flushed with nitrogen, **3d** (30 mg, 0.06 mmol) was dissolved in a THF/CH_2Cl_2 mixture (6:1, 3.5 mL). Then $[Pd(\eta^3\text{-}C_3H_5)(\mu\text{-}Cl)]_2$ (11 mg, 0.03 mmol) was added and the mixture was stirred at room temperature for 1 h. A sample of $AgBF_4$ (12 mg, 0.06 mmol) was added and the mixture was stirred in the dark for 24 h and then filtered off. The solvent was removed under reduced pressure. The product was dried under vacuum. The residue was washed with Et_2O (5 mL) and the desired Pd complex was recovered as a yellow solid by filtration (42 mg, 87%). ^{1}H NMR (CD_3CN, 300 MHz, 25 °C, TMS) appeared fluxional. IR (KBr): $\tilde{\nu}$ = 3250, 3100, 2928, 2859, 1610, 1461, 830, 802, 707 cm^{-1}. Crystals for structure determination were obtained by diffusion of *n*-hexane into a CH_2Cl_2 solution of [Pd(η^3-C_3H_5)-(**3d**)]BF_4. XRD details: Bruker APEX II CCD diffractometer (MoK_α radiation, λ 0.71073 Å), empirical absorption correction, anisotropic full-matrix least-squares on F^2. Results: $C_{29}H_{35}BF_4N_2PdS_4$, M_r = 733.04, monoclinic, space group C_2, *a* = 19.549(6), *b* = 9.652(2), *c* = 18.331(4) Å, β = 92.146(5)°, *V* = 3456.3(15) Å^3, *Z* = 4, ρ_x = 1.409 Mg m^{-3}, μ = 0.821 mm^{-1}, *F*(000) = 1496, *T* = 296(2) K, θ_{max} = 28.68°, 13138 reflections collected, 6919 with $I > 2\sigma(I)$. Final R_1 = 0.0627, wR_2 = 0.1829, GOF = 1.031, absolute structure parameter = 0.07(5).

[Pd(η^3-1,3-$Ph_2C_3H_3$)(3b)]BF_4: See ref. [13]. Crystals for X-ray diffraction were obtained by slow diffusion of *n*-hexane into an acetone solution of [Pd(η^3-1,3-Ph_2-C_3H_3)(**3b**)]BF_4. XRD details: Bruker AXS CCD diffractometer (MoK_α radiation, λ 0.71073 Å). Results: $C_{45}H_{51}BF_4N_2O_2PdS_4 \cdot 2(C_3H_6O)$, M_r = 973.33, orthorhombic, $P2_12_12_1$, *a* = 10.1154(15), *b* = 13.758(2), *c* = 33.294(5) Å, *V* = 4633.4(12) Å^3, *Z* = 4, ρ_x = 1.395 Mg m^{-3}, μ = 0.635 mm^{-1}, *F*(000) = 2008, *T* = 293(2) K, θ_{max} = 24.99°, 39545 reflections collected, 4425 with $I > 2\sigma(I)$. Final R_1 = 0.0957, wR_2 = 0.2215, GOF = 1.081, absolute structure parameter = 0.07(9).

Crystallographic data: CCDC 273523 and 273524 contain the supplementary crystallographic data for this paper. These data can be obtained free of charge from The Cambridge Crystallographic Data Centre via www.ccdc.cam.ac.uk/data request/cif/

Acknowledgements

This work was supported by M.I.U.R. (Rome), National Project "Stereoselezione in Sintesi Organica: Metodologie and Applicazioni", FIRB Project "Progettazione, preparazione e valutazione biologica e farmacologica di nuove molecole organiche quali potenziali farmaci innovativi," and by the University of Bologna. We are also indebted to "Graphilandia Media & Communication" (Taranto, Italy) for the striking artwork for the frontispiece. PRIN project "Nuove strategie per il controllo delle reazioni: interazione di frammenti molecolari con siti metallici in specie non convenzionali". FIRB project: Synthesis of novel organic materials and supramolecular architectures for high efficiency optoelectronics and photonic systems.

[1] I. Ojima, in *Catalytic Asymmetric Synthesis, Vol. II*, Wiley-VCH, New York, **2000**.
[2] *Comprehensive Asymmetric Catalysis* (Eds.: N. E. Jacobsen, A. Pfaltz, H. Yamamoto), Springer, Berlin, **1999**.
[3] R. Fiammengo, C. M. Bruinink, M. Crego-Calama, D. N. Reinhoudt, *J. Org. Chem.* **2002**, *67*, 8552–8557.
[4] a) M. McGarrigle, D. M. Murphy, D. G. Gilheany, *Tetrahedron: Asymmetry* **2004**, *15*, 1343–1354; b) P. B. Armstrong, L. M. Bennett, R. N. Constantine, J. L. Fields, J. P. Jasinski, R. J. Staples, R. C. Bunt, *Tetrahedron Lett.* **2005**, *46*, 1441–1445.
[5] For a recent example of chiral organometallic catalysis inspired to bio-catalyzed transformations, see: D. Magdziak, G. Lalic, H. M. Lee, K. C. Fortner, A. D. Aloise, M. D. Shair, *J. Am. Chem. Soc.* **2005**, *127*, 7284–7285.
[6] For a recent example of chiral organic catalysis inspired to bio-catalyzed transformations, see: S. G. Ouellet, J. B. Tuttle, D. W. C. MacMillan, *J. Am. Chem. Soc.* **2004**, *126*, 32–33.
[7] a) M. O. Wolf, *Adv. Mater.* **2001**, *13*, 545–553; b) B. J. Holliday, T. M. Swager, *Chem. Commun.* **2005**, 23–56.
[8] E. Holder, B. M. W. Langeveld, U. S. Schubert, *Adv. Mater.* **2005**, *17*, 1109–1121.
[9] a) D. Fichou, in *Handbook of Oligo- and Polythiophenes*, Wiley-VCH, Weinheim, **1999**; b) T. A. Skotheim, R. L. Elsenbaumer, J. R. Reynolds, in *Handbook of Conducting Polymers*, Marcel Dekker, New York, **1998**.
[10] a) S. Lamansky, P. Djurovich, D. Murphy, F. Adbel-Razzaq, R. Kwong, I. Tsyba, M. Bortz, B. Mui, R. Bau, M. E. Thompson, *Inorg. Chem.* **2001**, *40*, 1704–1711; b) S. Lamansky, P. Djurovich, D. Murphy, F. Abdel-Razzaq, H.-E. Lee, C. Adachi, P. E. Burrows, S. R. Forrest, M. E. Thompson, *J. Am. Chem. Soc.* **2001**, *123*, 4304–4312; c) C. Moorlag, M. O. Wolf, C. Bohne, B. O. Patrick, *J. Am. Chem. Soc.* **2005**, *127*, 6382–6393.
[11] a) L. Latos-Grazynski, J. Lisowski, P. Chmielewski, M. Grzeszczuk, M. M. Olmstead, A. L. Balch, *Inorg. Chem.* **1994**, *33*, 192–197; b) O. C. Clot, M. O. Wolf, B. O. Patrick, *J. Am. Chem. Soc.* **2001**, *123*, 9963–9973; c) X. Fang, J. G. Watkin, B. L. Scott, G. J. Kubas, *Organometallics* **2001**, *20*, 3351–3354; d) B.-F. Bonini, L. Giordano, M. Fochi, M. Comes-Franchini, L. Bernardi, E. Capitò, A. Ricci, *Tetrahedron: Asymmetry* **2004**, *15*, 1043–1051.
[12] *Palladium Reagents and Catalysis. New Perspectives for the 21st Century* (Ed.: J. Tsuji), Wiley, New York, **2004**.
[13] V. G. Albano, M. Bandini, M. Melucci, M. Monari, F. Piccinelli, S. Tommasi, A. Umani-Ronchi, *Adv. Synth. Cat.* **2005**, *347*, 1507–1512.
[14] S.-H. Kim, E.-K. Lee, G.-J. Kim, *Bull. Korean Chem. Soc.* **2004**, *25*, 754–756.
[15] B. M. Trost, D. L. Van Vraken, *Chem. Rev.* **1996**, *96*, 395–422.
[16] Phenomena of hemilability are frequently invoked in the rationalization of numerous organometallic catalyses. For a recent review regarding P/P(O) ligands, see: V. V. Grushin, *Chem. Rev.* **2003**, *103*, 1629–1662.
[17] Intramolecular Pd^0–HO interactions were recently reported on stabilizing Pd–BOX catalysts for AAA: K. Hallman, A. Frolander, T. Wondimagegn, M. Svensson, C. Moberg, *Proc. Natl. Acad. Sci. USA* **2004**, *101*, 5400–5404.
[18] J. Roncali, *Chem. Rev.* **1997**, *97*, 173–205.
[19] J. Casado, T. M. Pappenfus, L. L. Miller, K. R. Mann, E. Ortí, P. M. Viruela, R. Pou-Amérigo, V. Hernández, J. T. L. Navarrete, *J. Am. Chem. Soc.* **2003**, *125*, 2524–2534.
[20] H. Higuchi, Y. Uraki, H. Yokota, H. Koyama, J. Ojima, T. Wanda, H. Sasabe, *Bull. Chem. Soc. Jpn.* **1998**, *71*, 483–495.
[21] H.-P. Hu, H.-L. Chen, Z. Zheng, *Adv. Synth. Catal.* **2005**, *347*, 541–548.
[22] Unfortunately, the use of the pyrrolidine-based ligand **3f** in the AAA with **4c** was ruled out by formation, during the course of the reaction, of a dark brown, highly insoluble solid that removed the chiral Pd catalyst from the solution. Although a detailed investigation has not been performed so far, this peculiar behavior of **3f**

could be ascribed to a side interaction of the silver salt with the pyrrolidine units present in oligothienyl side arms.
[23] L. B. Groenendaal, F. Jonas, D. Freitag, H. Pielartzik, J. R. Reynolds, *Adv. Mater.* **2000**, *12*, 481–494.
[24] J.-M. Raimundo, P. Blanchard, P. Frère, N. Mercier, I. Ledoux-Rak, R. Hierle J. Roncali, *Tetrahedron Lett.* **2001**, *42*, 1507–1510.
[25] a) T. Yamagishi, M. Ohnuki, T. Kiyooka, D. Masai, K. Sato, M. Yamaguchi, *Tetrahedron: Asymmetry* **2003**, *14*, 3275–3279; b) B. M. Trost, A. C. Krueger, R. C. Bunt, J. Zambrano, *J. Am. Chem. Soc.* **1996**, *118*, 6520–6521; c) T. P. Clark, C. R. Landis, *J. Am. Chem. Soc.* **2003**, *125*, 11792–11793; d) O. Pàmies, M. Diéguez, C. Claver, *J. Am. Chem. Soc.* **2005**, *127*, 3646–3647.
[26] J. M. Canal, M. Gómez, F. Jiménez, M. Rocamore, G. Muller, E. Duñach, D. Franco, A. Jiménez, F. H. Cano, *Organometallics* **2000**, *19*, 966–978.
[27] a) P. R. Auburn, P. B. Mackenzie, B. Bosnich, *J. Am. Chem. Soc.* **1985**, *107*, 2033–2046; b) P. B. Mackenzie, J. Whelan, B. Bosnich, *J. Am. Chem. Soc.* **1985**, *107*, 2046–2054.
[28] a) P. Dierkes, S. Ramdeehul, L. Barloy, A. De Cian, P. C. J. Fisher, P. W. N. M. van Leeuwen, J. A. Osborn, *Angew. Chem.* **1998**, *110*, 3299–3301; *Angew. Chem. Int. Ed.* **1998**, *37*, 3116–3118; b) S. Ramdeehul, P. Dierkes, R. Aguado, P. C. J. Kamer, P. W. N. M. van Leeuwen, J. A. Osborn, *Angew. Chem.* **1998**, *110*, 3302–3304; *Angew. Chem. Int. Ed.* **1998**, *37*, 3118–3121.
[29] H. Steinhagen, M. Reggelin, G. Helmchen, *Angew. Chem.* **1997**, *109*, 2199–2202; *Angew. Chem. Int. Ed. Engl.* **1997**, *36*, 2108–2110.
[30] L. Canovese, G. Chessa, F. Visentin, P. Uguagliati, *Coord. Chem. Rev.* **2004**, *248*, 945–954.
[31] S. Bahmanyar, B. C. Borer, Y. M. Kim, D. M. Kurtz, S. Yu, *Org. Lett.* **2005**, *7*, 1011–1014.
[32] M. D'Auria, A. De Mico, F. D'Onofrio, G. Piancastelli, *J. Org. Chem.* **1987**, *52*, 5243–5247.
[33] Y. Zhang, A.-B. Hoernfeld, S. Gronowitz, *J. Heterocycl. Chem.* **1995**, *32*, 771–777.
[34] F. Effenberg, F. Würthner, F. Steybe, *J. Org. Chem.* **1990**, *55*, 2082–2091.
[35] M. M. M. Raposo, G. Kirsch, *Tetrahedron* **2003**, *59*, 4891–4899.
[36] P. von Matt, A. Pfaltz, *Angew. Chem.* **1993**, *105*, 614–615; *Angew. Chem. Int. Ed. Engl.* **1993**, *32*, 566–568.

Received: July 26, 2005
Published online: November 11, 2005

